

REPORT DOCUMENTATION PAGE			Form Approved OMB NO. 0704-0188		
<p>The public reporting burden for this collection of information is estimated to average 1 hour per response, including the time for reviewing instructions, searching existing data sources, gathering and maintaining the data needed, and completing and reviewing the collection of information. Send comments regarding this burden estimate or any other aspect of this collection of information, including suggestions for reducing this burden, to Washington Headquarters Services, Directorate for Information Operations and Reports, 1215 Jefferson Davis Highway, Suite 1204, Arlington VA, 22202-4302. Respondents should be aware that notwithstanding any other provision of law, no person shall be subject to any penalty for failing to comply with a collection of information if it does not display a currently valid OMB control number.</p> <p>PLEASE DO NOT RETURN YOUR FORM TO THE ABOVE ADDRESS.</p>					
1. REPORT DATE (DD-MM-YYYY) 03-09-2016		2. REPORT TYPE Final Report		3. DATES COVERED (From - To) 1-May-2013 - 30-Apr-2016	
4. TITLE AND SUBTITLE Final Report: A Novel Approach to Adaptive Flow Separation Control			5a. CONTRACT NUMBER W911NF-13-1-0122		
			5b. GRANT NUMBER		
			5c. PROGRAM ELEMENT NUMBER 206022		
6. AUTHORS Emmanuel G. Collins			5d. PROJECT NUMBER		
			5e. TASK NUMBER		
			5f. WORK UNIT NUMBER		
7. PERFORMING ORGANIZATION NAMES AND ADDRESSES Florida A&M University 1700 Lee Hall Drive 400 FHAC Tallahassee, FL 32307 -3200			8. PERFORMING ORGANIZATION REPORT NUMBER		
9. SPONSORING/MONITORING AGENCY NAME(S) AND ADDRESS (ES) U.S. Army Research Office P.O. Box 12211 Research Triangle Park, NC 27709-2211			10. SPONSOR/MONITOR'S ACRONYM(S) ARO		
			11. SPONSOR/MONITOR'S REPORT NUMBER(S) 62820-EG-REP.6		
12. DISTRIBUTION AVAILABILITY STATEMENT Approved for Public Release; Distribution Unlimited					
13. SUPPLEMENTARY NOTES The views, opinions and/or findings contained in this report are those of the author(s) and should not be construed as an official Department of the Army position, policy or decision, unless so designated by other documentation.					
14. ABSTRACT Due to their practical import, flow control problems have attracted increasing attention. This research specifically considers flow separation control, which can provide greater maneuverability and performance for the controlled system as well as reduced vibration. In particular, it considers control of flow separation over a NACA-0025 airfoil using microjet actuators and develops Adaptive Sampling Based Model Predictive Control (Adaptive SBMPC), a novel approach to Nonlinear Model Predictive Control that applies the Minimal Resource Allocation Network algorithm for nonlinear system identification and the Sampling Based Model Predictive Optimization (SBMPO).					
15. SUBJECT TERMS nonlinear model predictive control, adaptive control, flow control, nonlinear systems, neural networks, graph search, nonlinear optimization					
16. SECURITY CLASSIFICATION OF:			17. LIMITATION OF ABSTRACT UU	15. NUMBER OF PAGES	19a. NAME OF RESPONSIBLE PERSON Emmanuel Collins
a. REPORT UU	b. ABSTRACT UU	c. THIS PAGE UU			19b. TELEPHONE NUMBER 850-410-6367

## Report Title

Final Report: A Novel Approach to Adaptive Flow Separation Control

### ABSTRACT

Due to their practical import, flow control problems have attracted increasing attention. This research specifically considers flow separation control, which can provide greater maneuverability and performance for the controlled system as well as reduced vibration. In particular, it considers control of flow separation over a NACA-0025 airfoil using microjet actuators and develops Adaptive Sampling Based Model Predictive Control (Adaptive SBMPC), a novel approach to Nonlinear Model Predictive Control that applies the Minimal Resource Allocation Network algorithm for nonlinear system identification and the Sampling Based Model Predictive Optimization (SBMPO) algorithm to achieve effective nonlinear control. Through pressure data and flow characterization from wind tunnel experiments, effective and robust separation control is demonstrated and it is seen that the method's computational efficiency is sufficient for successful real time implementation. Furthermore, this research shows that SBMPC is guaranteed to find the global minimum subject to the sampling if the prediction horizon is sufficiently long. On problems of increasingly complexity it is demonstrated to avoid the local minima to which gradient-based methods tend to converge and is also shown to be effective with a multi-input, multi-output, time-varying power system combustion control problem.

---

**Enter List of papers submitted or published that acknowledge ARO support from the start of the project to the date of this printing. List the papers, including journal references, in the following categories:**

**(a) Papers published in peer-reviewed journals (N/A for none)**

<u>Received</u>	<u>Paper</u>
-----------------	--------------

**TOTAL:**

**Number of Papers published in peer-reviewed journals:**

---

**(b) Papers published in non-peer-reviewed journals (N/A for none)**

<u>Received</u>	<u>Paper</u>
-----------------	--------------

**TOTAL:**

**Number of Papers published in non peer-reviewed journals:**

---

**(c) Presentations**

Number of Presentations: 0.00

Non Peer-Reviewed Conference Proceeding publications (other than abstracts):

Received Paper

TOTAL:

Number of Non Peer-Reviewed Conference Proceeding publications (other than abstracts):

Peer-Reviewed Conference Proceeding publications (other than abstracts):

Received Paper

09/03/2016 1.00 Farrukh S. Alvi, Brandon M. Reese, Emmanuel G. Collins. A Nonlinear Adaptive Method for Microjet-Based Flow Separation Control, 7th AIAA Flow Control Conference. 16-JUN-14, Atlanta, GA. : ,

TOTAL: 1

Number of Peer-Reviewed Conference Proceeding publications (other than abstracts):

(d) Manuscripts

Received Paper

08/02/2016 4.00 . A graph search and neural network approach to adaptive nonlinear model predictive control, Engineering Applications of Artificial Intelligence ( )

TOTAL: 1

Number of Manuscripts:

Books

Received      Book

TOTAL:

Received      Book Chapter

TOTAL:

Patents Submitted

ADAPTIVE NONLINEAR MODEL PREDICTIVE CONTROL USING A NEURAL NETWORK AND INPUT  
—SAMPLING—

Patents Awarded

Awards

Black Engineer of the Year Award for College-Level Promotion of Education, February 2015.  
ASME Fellow, April 2013.

Graduate Students

<u>NAME</u>	<u>PERCENT SUPPORTED</u>	Discipline
Brandon Reese	0.30	
Kevin Powell	0.20	
<b>FTE Equivalent:</b>	<b>0.50</b>	
<b>Total Number:</b>	<b>2</b>	

Names of Post Doctorates

<u>NAME</u>	<u>PERCENT SUPPORTED</u>
Brandon Reese	0.80
<b>FTE Equivalent:</b>	<b>0.80</b>
<b>Total Number:</b>	<b>1</b>

---

### **Names of Faculty Supported**

<u>NAME</u>	<u>PERCENT SUPPORTED</u>	National Academy Member
Emmanuel Collins	0.05	
Farrukh Alvi	0.05	
<b>FTE Equivalent:</b>	<b>0.10</b>	
<b>Total Number:</b>	<b>2</b>	

---

### **Names of Under Graduate students supported**

<u>NAME</u>	<u>PERCENT SUPPORTED</u>
<b>FTE Equivalent:</b>	
<b>Total Number:</b>	

### **Student Metrics**

This section only applies to graduating undergraduates supported by this agreement in this reporting period

The number of undergraduates funded by this agreement who graduated during this period: ..... 0.00

The number of undergraduates funded by this agreement who graduated during this period with a degree in science, mathematics, engineering, or technology fields:..... 0.00

The number of undergraduates funded by your agreement who graduated during this period and will continue to pursue a graduate or Ph.D. degree in science, mathematics, engineering, or technology fields:..... 0.00

Number of graduating undergraduates who achieved a 3.5 GPA to 4.0 (4.0 max scale):..... 0.00

Number of graduating undergraduates funded by a DoD funded Center of Excellence grant for Education, Research and Engineering:..... 0.00

The number of undergraduates funded by your agreement who graduated during this period and intend to work for the Department of Defense ..... 0.00

The number of undergraduates funded by your agreement who graduated during this period and will receive scholarships or fellowships for further studies in science, mathematics, engineering or technology fields: ..... 0.00

---

### **Names of Personnel receiving masters degrees**

<u>NAME</u>
<b>Total Number:</b>

---

### **Names of personnel receiving PHDs**

<u>NAME</u>
Brandon Reese
<b>Total Number:</b>

---

### **Names of other research staff**

<u>NAME</u>	<u>PERCENT SUPPORTED</u>
<b>FTE Equivalent:</b>	
<b>Total Number:</b>	

---

### **Sub Contractors (DD882)**

## **Inventions (DD882)**

## Scientific Progress

## Abstract

Due to their practical import, flow control problems have attracted increasing attention. This research specifically considers flow separation control, which can provide greater maneuverability and performance for the controlled system as well as reduced vibration. In particular, it considers control of flow separation over a NACA-0025 airfoil using microjet actuators and develops Adaptive Sampling Based Model Predictive Control (Adaptive SBMPC), a novel approach to Nonlinear Model Predictive Control that applies the Minimal Resource Allocation Network algorithm for nonlinear system identification and the Sampling Based Model Predictive Optimization (SBMPO) algorithm to achieve effective nonlinear control. Through pressure data and flow characterization from wind tunnel experiments, effective and robust separation control is demonstrated and it is seen that the method's computational efficiency is sufficient for successful real time implementation. Furthermore, this research shows that SBMPC is guaranteed to find the global minimum subject to the sampling if the prediction horizon is sufficiently long. On problems of increasingly complexity it is demonstrated to avoid the local minima to which gradient-based methods tend to converge and is also shown to be effective with a multi-input, multi-output, time-varying power system combustion control problem.

## List of Illustrations

1. Block Diagram of Adaptive SBMPC
2. Airfoil Schematic
3.  $Z_{\text{lift}}$  Performance Function
4. Experimental Comparison of  $Z_{\text{lift}}$  and Coefficient of Lift
5. Lift Control - Closed Loop Case 1
6. Lift Control - Closed Loop Case 2
7. Lift Control - Closed Loop Case 3
8. Lift Control - Closed Loop Case 4
9. Lift Control - Closed Loop Case 5
10. PIV Visualization Uncontrolled and Controlled Cases: angle of attack  $16^\circ$ , velocity 15 m/s
11. PIV Visualization Uncontrolled and Controlled Cases: angle of attack  $22^\circ$ , velocity 11 m/s
12. Rastigrin's Function in One Dimension
13. MPC Convergence Behavior Summary
14. Benchmark Plant Visualization
15. Benchmark Results:  $\beta = 0.2$ , step tracking
16. Time Variation of Simulation Plant Dynamics for the Power System Combustion Control Problem
17. Neural GPC Power Plant Combustion Control Results
18. SBMPC Power Plant Combustion Control Results

## Statement of the Problem Studied

The closed loop control of flow separation in changing environments presents a significant challenge due to unknown, nonlinear system dynamics, and changing flow conditions. Currently available methods have produced good results for static flow conditions, but they require excessive tuning and therefore are not robust to changes such as angle of attack or Reynolds Number variation. This research investigates a new approach to flow control based on adaptive, neural network modeling and graph search optimization. The approach is called Adaptive Sampling Based Model Predictive Control (Adaptive SBMPC) and is illustrated in Fig. 1. It is developed to enable adaptive nonlinear control of systems that can converge to near global minimum and enables enforcement of constraints on both the system inputs and outputs. The research considers control of flow separation over a NACA-0025 airfoil using microjet actuators and pressure transducers as illustrated in Fig. 2. It is also sought to develop algorithm completeness theory for the control optimization that is a key element of Adaptive SBMPC and illustrate the power of SBMPC to avoid local minima, a feature not shared by gradient-based optimization methods.

## Summary of the Most Important Results

### Development of a lift performance function [1]

To develop a nonlinear adaptive control method for flow separation control first required the development of a performance function that is based on the available pressure measurements and can approximate lift, the variable to be manipulated in this research. Hence, the first contribution of this research was to develop  $Z_{\text{lift}}$  as an approximation of  $C_L$ , the non-dimensional lift coefficient. Fig. 3 shows how  $Z_{\text{lift}}$  was computed in this research while Fig. 4 shows the close correspondence between  $Z_{\text{lift}}$  and  $C_L$  in actual experiments.



## Experiments that demonstrate control of lift [1,2]

The experiments were conducted using a subsonic wind tunnel. A section of a NACA 0025 airfoil was fitted with pressure transducers as shown in Fig. 2. As discussed above, the four pressure transducers along the center chord were used to approximate lift on the airfoil and to detect changes in lift due to separation. Microjets were drilled near the leading edge as a means of actuation, and the blowing pressure supplied to these microjets is the actuation input used to control separation. Before each closed loop control experiment, there was an open loop training phase, in which a sweep of input frequencies are commanded. From the measured outputs, a model was constructed that represents the relationship between inputs and outputs of the plant. After the training phase, the neural network was continually updated and could therefore adjust to both small and large changes in plant behavior.

The closed-loop experimental results demonstrate the capability to not only maximize lift, but also control lift by commanding intermediate values. In Fig. 5, the commanded reference signal (dashed line) is constant, which means the control system was configured to increase and hold  $Z_{\text{lift}}$  constant. The actual output signal (solid line) achieves the commanded increase-and-hold behavior. In Fig. 6, the commanded reference was manually stepped downwards, in order to demonstrate the ability of the control system to decrease  $Z_{\text{lift}}$  when desired. Fig 7 displays similar results and includes both upward and downward stepwise motion. For the case shown in Fig 8, the neural network was trained at a Reynolds number of 125,000, but control is demonstrated for a Reynolds number of 150,000. Some prediction error, indicated by the departure of the dotted line from the solid line, occurs around 13 seconds, but the error is corrected within 5 seconds. This demonstrates the robustness achieved by online system identification.

Fig. 9 shows the control adjustment in reaction to changes in Reynolds number during operation. The system adjusts the neural network model at the same time as the updated control signal is being computed and executed. The adaptation of the neural network model is vital when flow conditions change. In Fig. 9, the model adaptation is what allows the neural net prediction signal (dotted curve) to adjust to match the measured signal (solid curve) even when the flow conditions change. SBMPC is then responsible for modifying the control input signal so that the prediction signal matches the reference signal (dashed curve). Because of the closed loop control system, it was possible to take a scenario where the flow was controlled and attached, change the wind tunnel speed so that the flow separates, and observe the neural network adaptation and controller reaction as the flow is automatically reattached. The 15-second transient beginning at the 10 second mark is a model adaptation, not a transient on control. While the model has moderate error, the control system continues to operate, but may be less efficient until this adaptation is complete.

In order to verify that the changes in  $Z_{\text{lift}}$  actually correspond to a changing degree of separation in the flow, visualization experiments were performed to capture the velocity field surrounding the wing both with and without control enabled. In these experiments, the airfoil wind tunnel configuration was fixed to a particular angle of attack and tunnel velocity. The velocity field was then measured via Partial Image Velocimetry (PIV) and averaged over a 1000-frame, 60-second window. For the purpose of visualization, the image processing results are displayed with a flipped y-axis so that the angle of attack is depicted as positive. (The PIV experiments were performed with a negative angle of attack.) The control system was then enabled to maximize  $Z_{\text{lift}}$ . The control system can be configured to maximize lift by prescribing a constant reference trajectory that is greater than the attainable range of  $Z_{\text{lift}}$  values. In this case, the reference for  $Z_{\text{lift}}$  was set to 0. A second series of PIV measurements of the same duration was collected to characterize the controlled flow. Contours of streamwise velocity  $V_x$  are shown in Figs. 10 and 11, and display the uncontrolled and controlled flows for two different flow conditions (angle of attack 16 deg, Re 150,000, and angle of attack 22 deg, Re 90,000, respectively) when the controller is set to maximize  $Z_{\text{lift}}$ . In the absence of blockage effects and for a larger PIV window, the value of  $V_x/V_{\infty}$  would equal 1 far from the airfoil. In these figures, the separated region is outlined by zero-velocity contours shown in black. Based on averaged pressure data, the enabling of control increased average  $Z_{\text{lift}}$  by 1.4 and 1.7 respectively. In both cases, the separation bubble is greatly reduced in size and is further downstream. The flow fields indicate massive separation when uncontrolled, and while there is some separation with control, the size of the trailing edge separated region is less, indicating the limitations of the actuators' control authority.

In summary, the experimental results show that the closed loop control system using Adaptive SBMPC was not only able to reattach separated flow, it also controlled the degree of separation when required. The result was the ability to command lift and adapt to changes in the flow conditions. Control was achieved in real time, demonstrating that Adaptive SBMPC is computationally efficient enough to perform active control on time scales on the order of 100 ms. (The identification and control algorithms were programmed in C and implemented in a real time environment on dSPACE 1006 hardware.)

## SBMPC Completeness [3]

For the receding horizon MPC problem, we define a goal state as any horizon-depth node whose trajectory is minimal in cost. A {sound} graph search algorithm returns only trajectory solutions that reach a goal state. A given sound algorithm is {complete} if it always returns one such solution if any solution exists. Assuming the heuristic function (i.e., the prediction of the cost to move from the current state to the goal state that is used by SBMPC) always underestimates the lowest cost to the prediction horizon, SBMPC (the optimization that underlies the control portion of Adaptive SBMPC), like A\* and other graph search algorithms, may be shown to be complete over a given graph. A proof was formally derived in this research. It guarantees that subject to

sufficient depth and breadth of sampling, SBMPO will find a globally optimal solution. Due to gaps between samples, some suboptimality will result.

Demonstration that SBMPC can avoid local minima and converge to or near the global minimum [3]

SBMPC was applied to finding the optimal of Rastrigin's function, which as shown in Fig. 12 has numerous local minima. As shown in Fig. 13(a) SBMPC always converged to the global minimum, independent of the initial conditions. In contrast, Fig. 13 (b) shows that Sequential Quadratic Programming (SQP) MPC only converges to the local minimum when the initial state is near the global minimum.

A more complex benchmark dynamic system characterized by a parameter  $\beta$  was also considered. As shown in Fig. 14(a), when  $\beta = 1.0$ , the plant has few local minima. However, Fig. 14(b) shows that when  $\beta = 0.2$ , the plant has numerous local minima. For the latter case Fig. 5 shows that due to the presence of the local minima SBMPC was able to outperform Generalized Predictive Control (GPC), an established method for NMPC that relies on gradient-based optimization.

Comparison between Adaptive SBMPC and Neural GPC in a power plant combustion application [3]

To consider adaptive control of a complex multiple input – multiple output system, a comparison between Adaptive SBMPC and the Neural GPC methods was performed with a simulated power plant combustion control example. When controlling a combustion system, constraints on inputs and outputs are necessary in order to meet power demands, ensure safe operating levels, or regulate environmental pollutants. For these reasons, the industry's need for handling these constraints has steadily increased, and MPC is arguably the control methodology most suitable to handle them. For the problem considered in this research, the inputs are fuel mass rate ( $u_1$ ) and oxygen damper angle ( $u_2$ ), and the outputs to be controlled are the flue volume concentrations of oxygen, carbon dioxide, and carbon monoxide.

In the simulation, plant dynamics are applied as step parameter changes at the beginning of each 500 second interval of simulation time. The nature of the changing boiler dynamics is presented in Fig. 16. Each change is from the normal dynamic behavior, such that the changes mentioned are in effect during the interval but revert back to the normal values.

The data for the case shown in Figs. 17 and 18 indicates that after each shift in plant dynamics, the neural networks are adapted and prediction errors were corrected. In Figure 17 Neural GPC exhibited significant and sustained tracking error due to violation of the  $u_2$  input constraint. (Neural GPC does not guarantee enforcement of the input constraints.) Fig. 18 shows that SBMPC did not violate the input constraints and achieved strong tracking behavior. After each plant change, the neural networks quickly adapt to decrease the prediction error.

## Concluding Remarks

Adaptive Sampling Based Model Predictive Control (Adaptive SBMPC) has been developed and implemented in both experiments and simulations. The method has a strong theoretical foundation and has the clear advantage over gradient-based methods of having the ability to avoid local minimum as illustrated in simulated examples. The application to flow separation control shows the great promise of this method for real time implementation in real world applications. Closed loop control of separated flows has been demonstrated using this new approach. Quantitative results using a pressure-based lift approximation indicate the effectiveness of the control system to control flow behavior based on a nonlinear neural network model constructed from data. This model is adjusted in real time to represent changes in flow conditions while the controller is in operation. The closed loop experiments demonstrated successful tracking of desired values of  $Z_{lift}$  by mitigating flow separation. The control system is able to increase or decrease lift in response to an external command, subject to the limitations of the actuator. Both the nonlinear input-to-output behavior of the system and the nonlinear control law are learned adaptively, so even when flow conditions were modified during a control experiment, the control system was successful in adjusting the inputs to meet the desired  $Z_{lift}$  value. A few selected cases were visualized using PIV, which verified the reduction in flow separation.

The nonlinear system identification and control technique developed in this research requires few tuning parameters, making it easily applicable to many other configurations of sensors and actuators beyond the unsteady pressure transducer and microjet configuration initially considered. This implementation of Adaptive SBMPC is the first to demonstrate flow separation control using a model that is nonlinear and updated online.

The SBMPO algorithm used for control optimization is shown via mathematical proof to be a complete search algorithm subject to sufficient sampling density and length of the prediction horizon. Hence, unlike approaches that optimize by linearization, convergence to a nearly global minimum is achievable even when numerous local minima exist. This is first demonstrated with a global optimization of Rastrigin's Function, where SBMPC is shown to outperform MPC based on Sequential Quadratic Programming optimization. It was also demonstrated using another benchmark problem from the literature, and SBMPC was shown to outperform the established NMPC technique, Neural GPC, in avoiding local minima.

Adaptive SBMPC and Neural GPC control systems were further used to perform Adaptive NMPC. The results of this research indicate that both neural network structures are capable of representing the nonlinear system and both control methodologies easily handle the SISO time-invariant control case. The results of this research are the first control results to use Neural GPC to control a time-varying MIMO plant. However, when a MIMO power plant combustion control problem was considered, Neural GPC tended to violate the input constraints, which led to poor reference tracking. By design, Adaptive SBMPC cannot violate input constraints and good tracking results were achieved.

Simulation results with the combustion control problem were presented for changing dynamics and highlight the adaptive nature of the control system as did some of the flow separation control results. One limitation of these and other NMPC approaches is the breakdown due to complexity for large numbers of inputs and outputs. However, SBMPC is naturally compatible with parallel computations since it uses a divide-and-conquer approach to perform optimization. Node expansion is the most costly portion of the Adaptive SBMPC algorithm, but these computations can be implemented in parallel. There is also a possibility for significant computational improvement with the addition of search heuristics and a parallel implementation of portions of the algorithm. Within a graph search optimization, a suitable heuristic can dramatically reduce the number of nodes that are expanded, and performing the edge cost calculation in parallel on multiple cores could significantly reduce the required run time per node.

In summary, the results of this research have resulted in a novel and widely applicable adaptive nonlinear control methodology. It is expected to find many additional applications in flow control and other fields such as power system control and automotive engine tuning.

## References

1. B. Reese, F. Alvi, and E. G. Collins, "A Nonlinear Adaptive Method for Microjet-Based Flow Separation Control," 7th AIAA Flow Control Conference, Atlanta, GA, June 16 – 20, 2014.
2. B. Reese, E. G. Collins, Jr., and F. Alvi, "A Nonlinear Adaptive Method for Microjet-Based Flow Separation Control," AIAA Journal, to appear, available at <http://arc.aiaa.org/doi/10.2514/1.J054307>.
3. B. Reese and E. G. Collins, Jr., "A Graph Search and Neural Network Approach to Adaptive Nonlinear Model Predictive Control," Engineering Applications of Artificial Intelligence, Vol. 55, 2016, pp. 250-268.

## Technology Transfer

Funded collaboration with Siemens Corporation on project entitled, "Adaptive Sampling Based Model Predictive Control for the Ammonia Feed System of the Selective Catalytic Reduction (SCR) System in a Combined Cycle Plant".

NASA SBIR with Spectral Energies, LLC on project entitled, "Flow Control on a High Lift Airfoil Using High-Bandwidth Microactuators".

DOE STTR with Nhu Energy, Inc., entitled "Optimal Integrated Control of Grid-Connected PV Generation and On-site-Load".

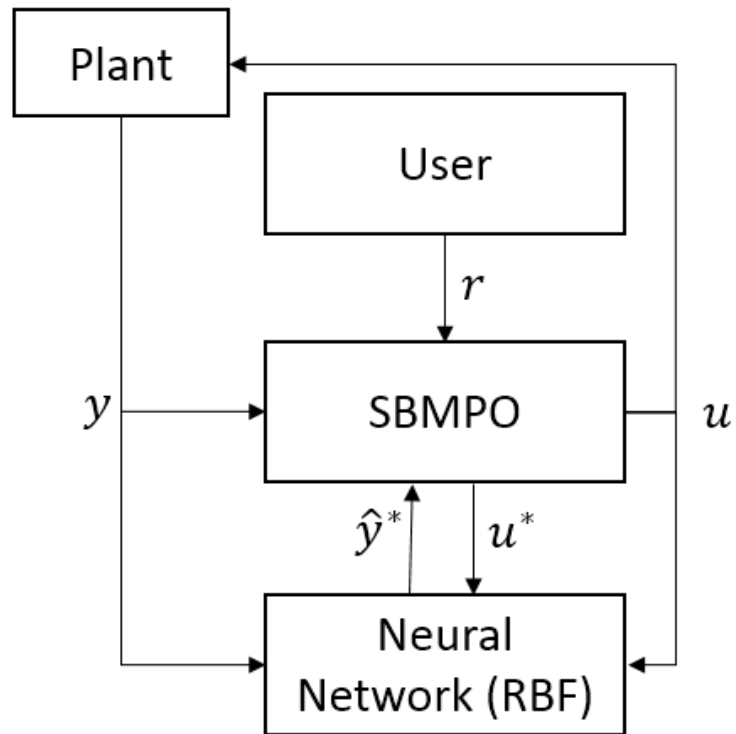


Figure 1. Block diagram of Adaptive SBMPC. The control task is to provide inputs  $u$  to the plant such that outputs  $y$  match a reference trajectory  $r$ . The neural network model is identified online, and as candidate input trajectories  $u^*$  are provided by SBMPO to the neural network, their corresponding predicted outputs  $\hat{y}^*$  are returned.

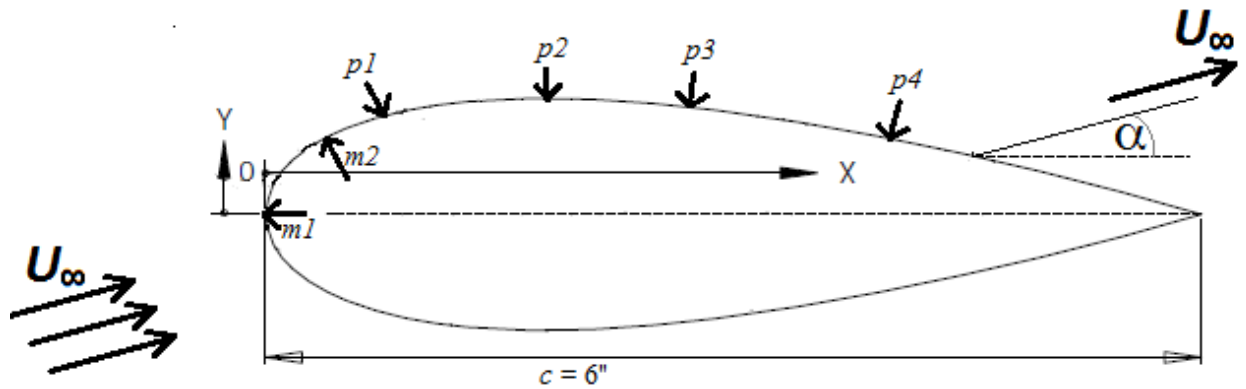
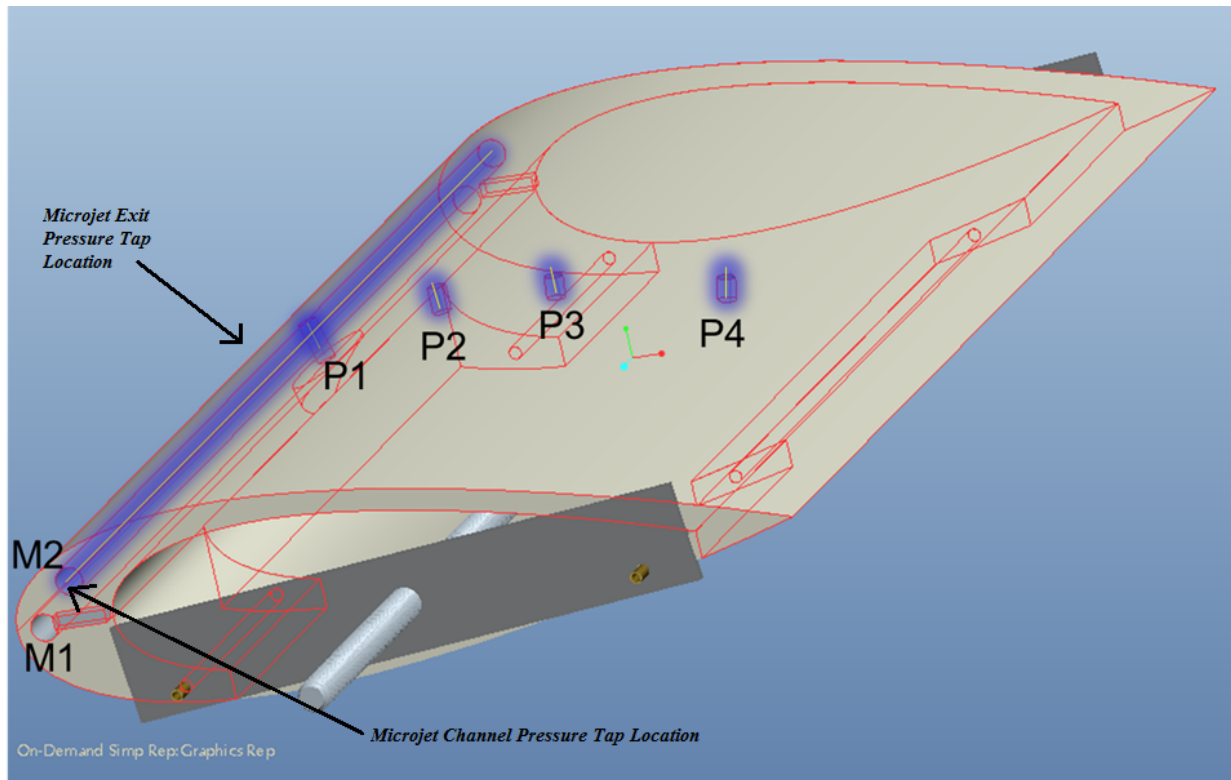


Figure 2. Airfoil Schematic. The (top) diagram includes microjet array and pressure transducer locations. The pressure transducers at four distinct locations give enough information about the surface pressure distribution to approximate lift changes. The cross section schematic (lower) is also shown.

$$Z_{lift} = \frac{\sum_{i=1}^N w_i p_i}{\frac{1}{2} \rho V_{\infty}^2}$$

$V_{\infty}$  is the freestream velocity.

Symbol	Parameter	Value(s)
$w_1$	$p_1$ Weight	-1.000
$w_2$	$p_2$ Weight	-0.9781
$w_3$	$p_3$ Weight	-0.9348
$w_4$	$p_4$ Weight	-0.9126

Figure 3.  $Z_{lift}$  Performance Function.  $Z_{lift}$  was used in this research to approximate the lift coefficient. It is computed using the four pressure measurements of Figure 2.

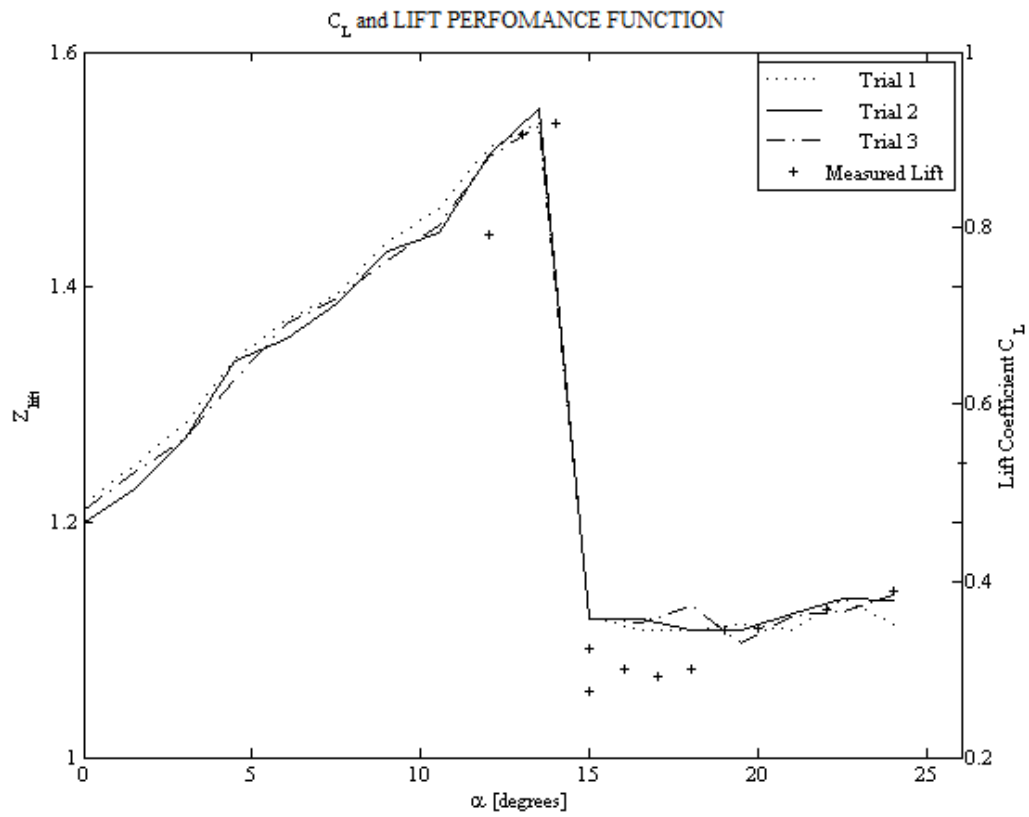


Figure 4. Experimental Comparison of  $Z_{lift}$  and Coefficient of Lift. For  $RE = 95,000$ , computed  $Z_{lift}$  values are plotted with experimentally measured  $C_L$  (lift coefficient) values vs. the angle of attack  $\alpha$ .

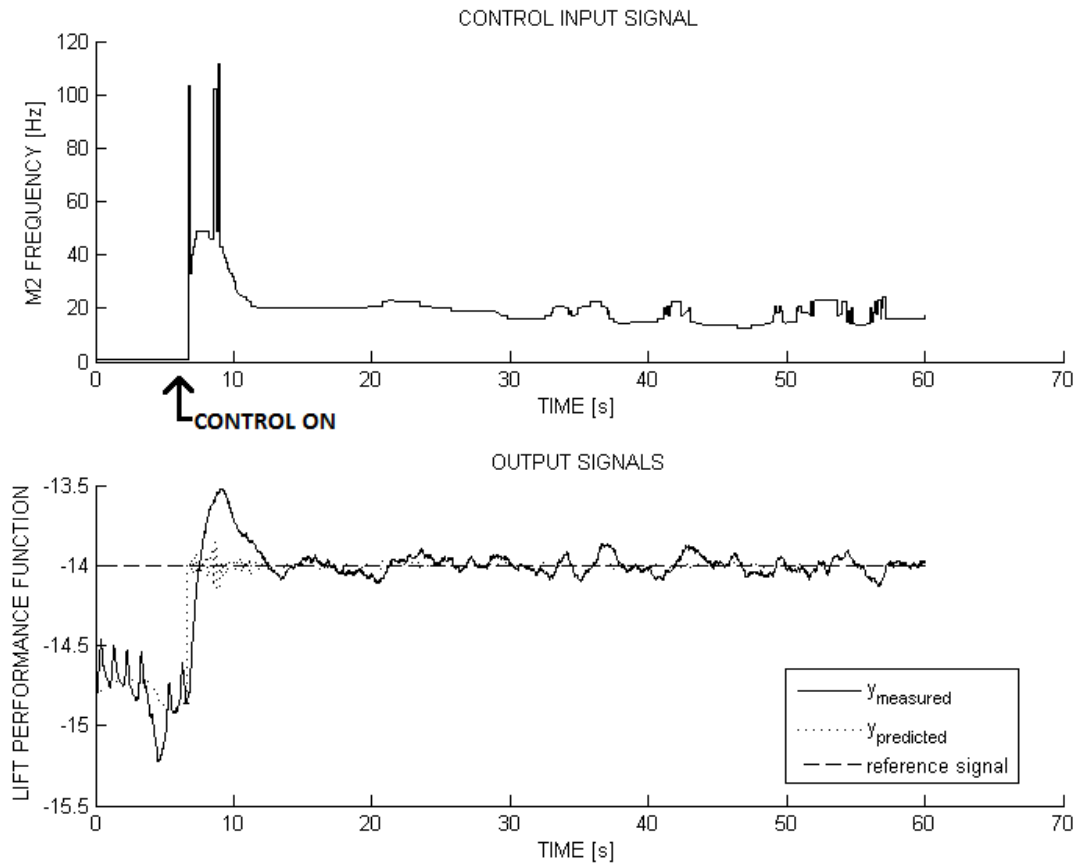


Figure 5. Lift Control - Closed Loop Case 1: The Reynolds number is 125,000, and the angle of attack is  $20^\circ$ . This closed loop case illustrates the ability to follow a step reference signal subsequent to the activation of the SBMPC controller.



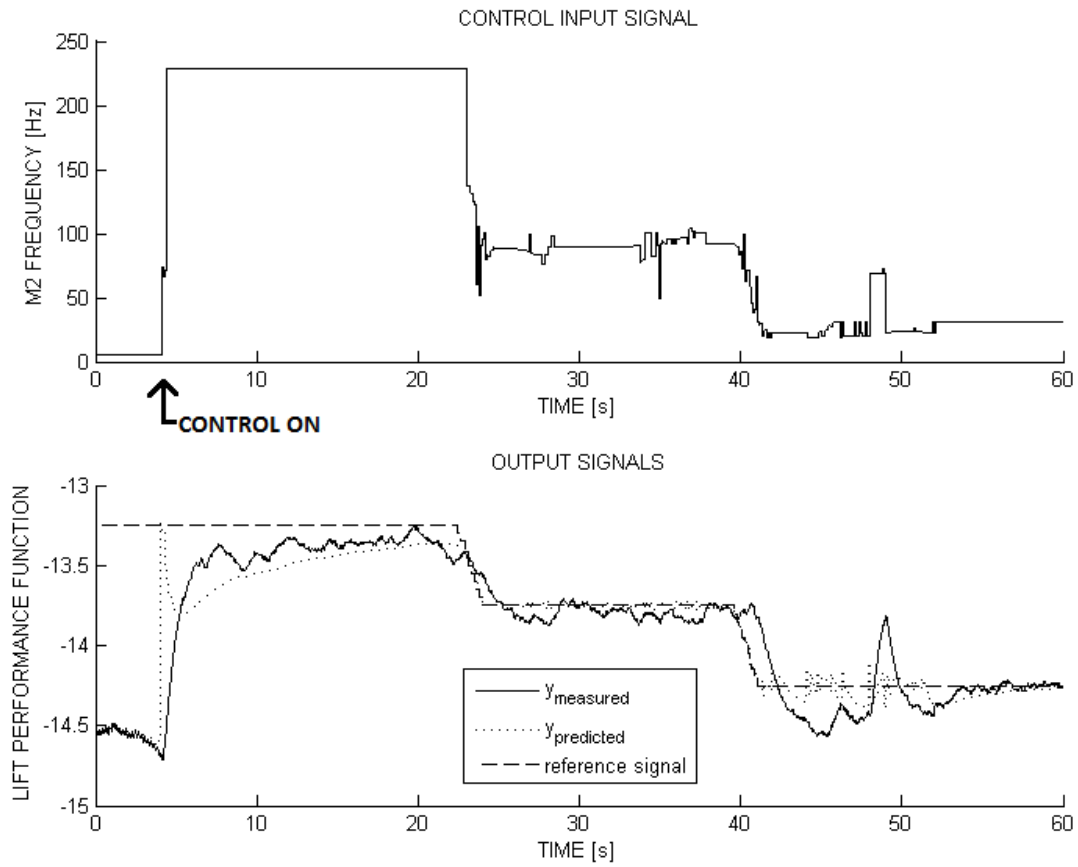


Figure 6. Lift Control - Closed Loop Case 2: The Reynolds number is 125,000, and the angle of attack is  $20^\circ$ . This closed loop case illustrates the ability to command intermediate values of  $Z_{\text{lift}}$ .

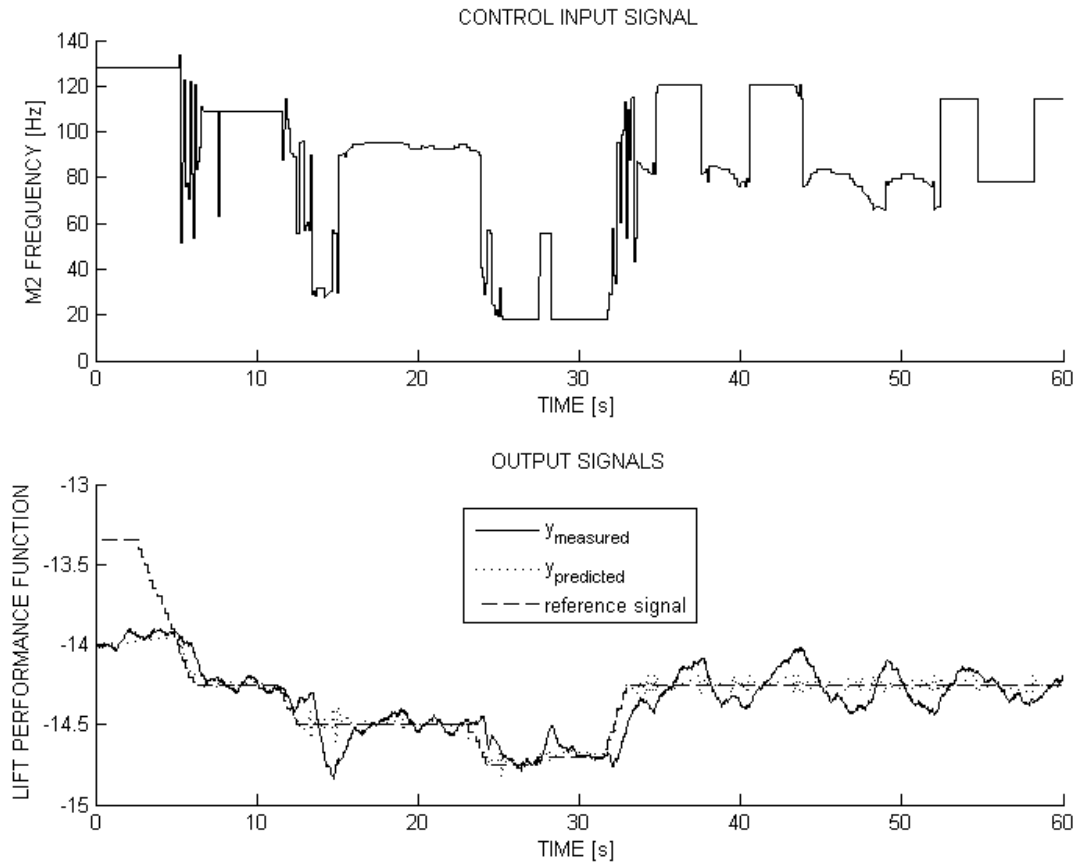


Figure 7. Lift Control - Closed Loop Case 3: The Reynolds number is 125,000, and the angle of attack is  $20^\circ$ . This closed loop case illustrates the saturation behavior of the controller: from time 0 to 5 seconds,  $Z_{\text{lift}}$  is simply maximized when the specified reference is above the attainable actuation range. Tracking resumes when the reference value is decreased to an attainable value.

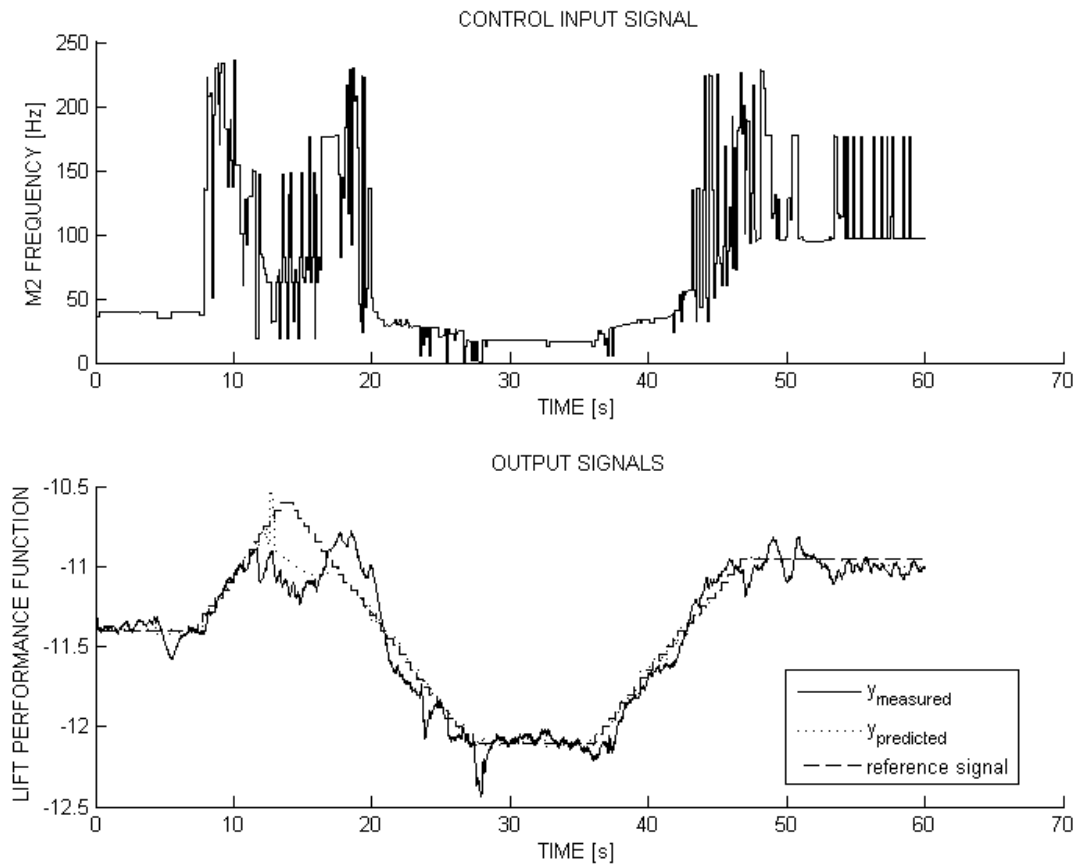


Figure 8. Lift Control - Closed Loop Case 4: The Reynolds number is 150,000, and the angle of attack is  $20^\circ$ . This closed loop case illustrates the ability to track ramp trajectories. During training, the tunnel Reynolds number was set to 125,000, ensuring that online model adaptation would be required when tested at a higher Reynolds number.

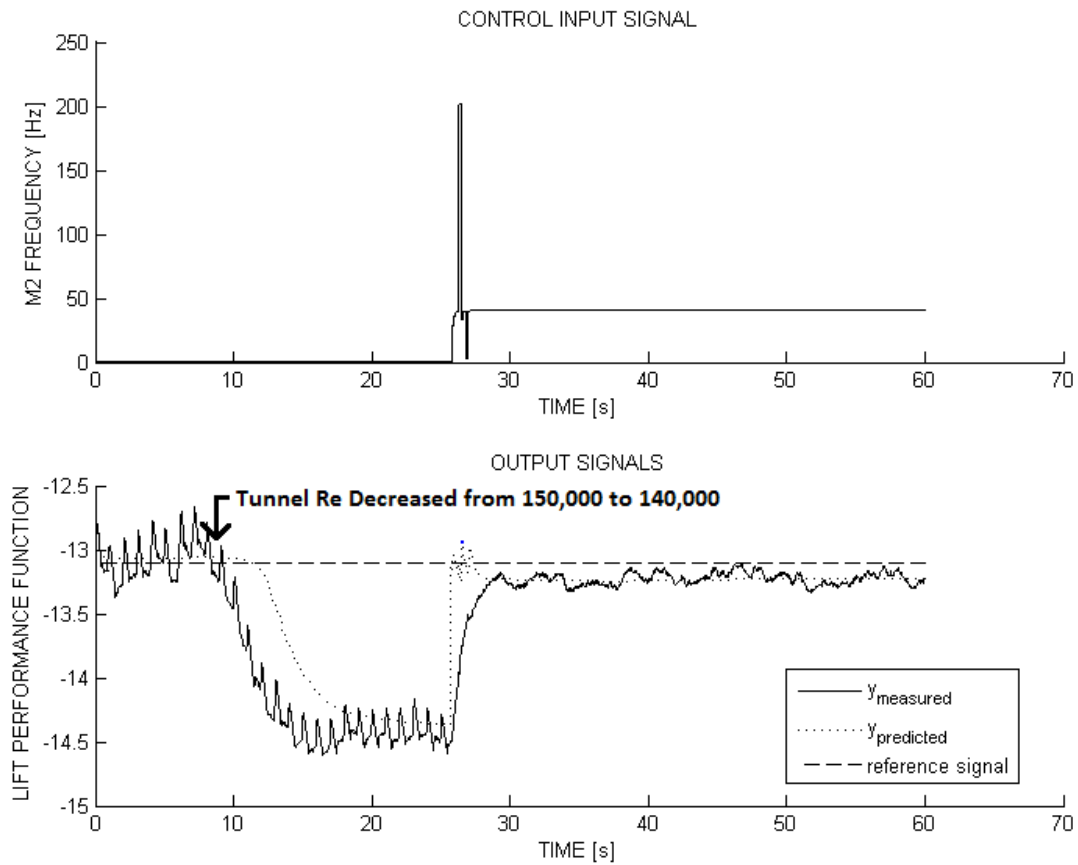
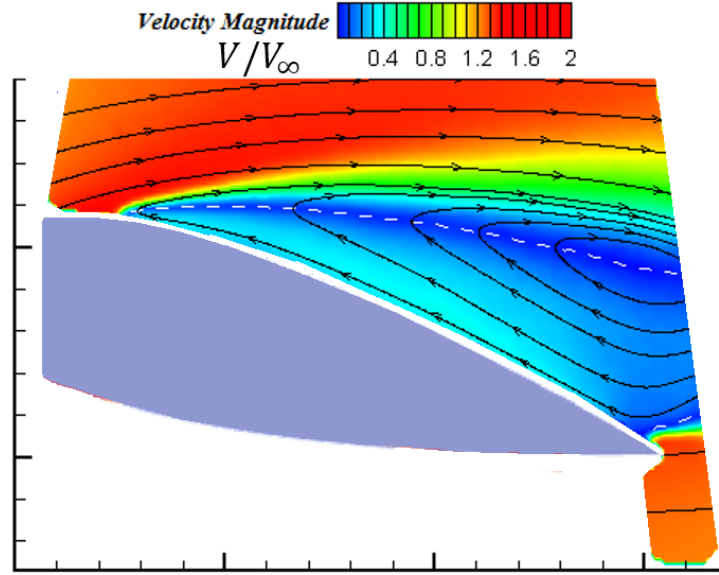
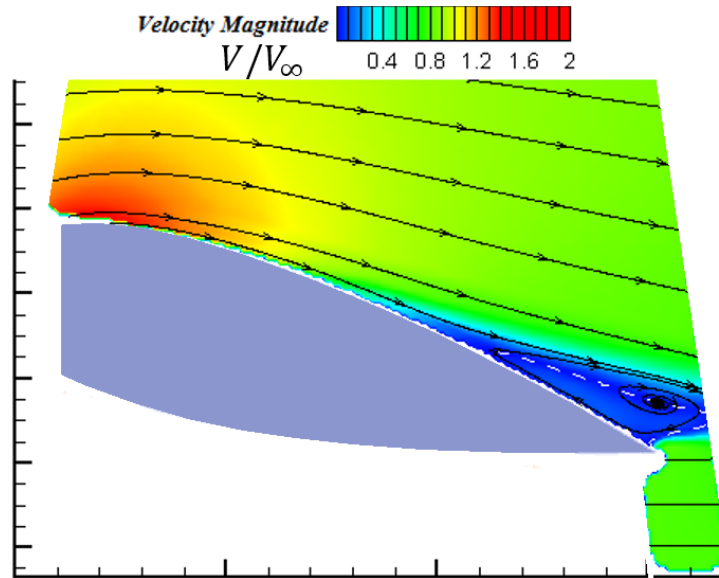


Figure 9. Lift Control - Closed Loop Case 5: The Reynolds number shifts from 150,000 to 140,000, and the angle of attack is  $20^\circ$ . This case demonstrates that the ability to adapt enables the control system to be robust to changes in the flow conditions.

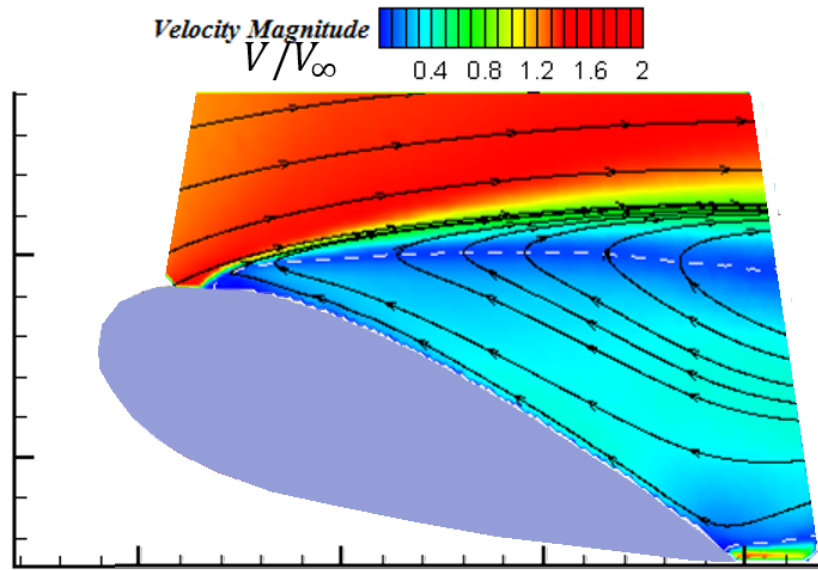


(a)

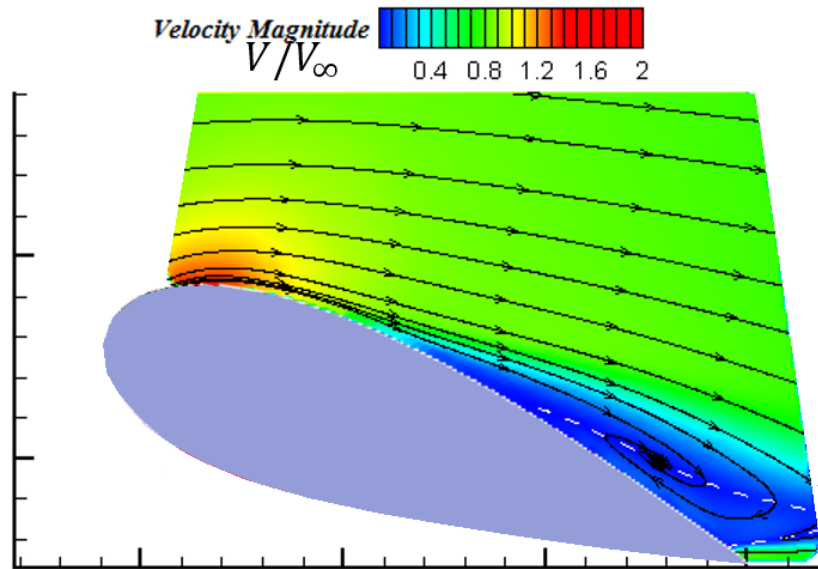


(b)

Figure 10. PIV Visualization Uncontrolled and Controlled Cases: angle of attack  $16^\circ$ , velocity 15 m/s. The PIV data in (a) was collected with the control system off, the data in (b) was collected with the control system set to maximize  $Z_{lift}$ , and the tunnel speed corresponds to a Reynolds number of 150,000 based on chord length. The white dashed line indicates zero horizontal velocity  $V_x$ .

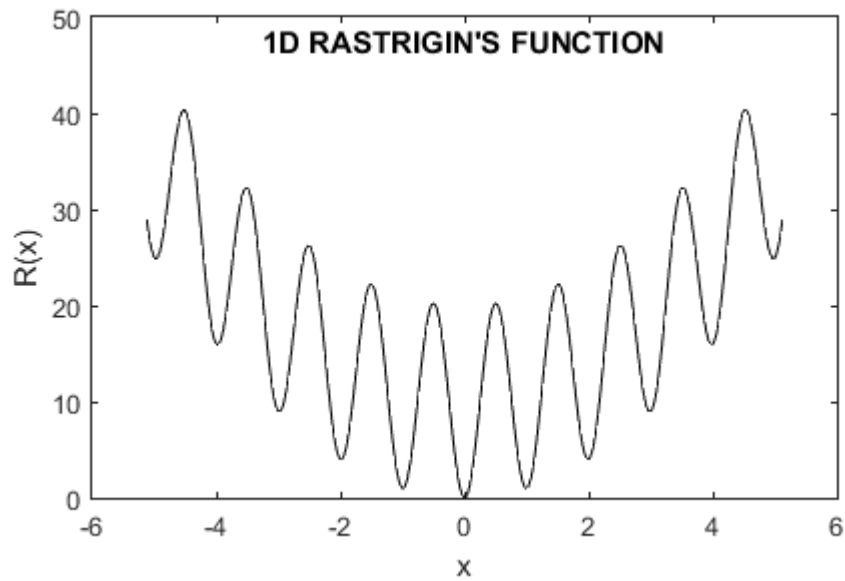


(a)

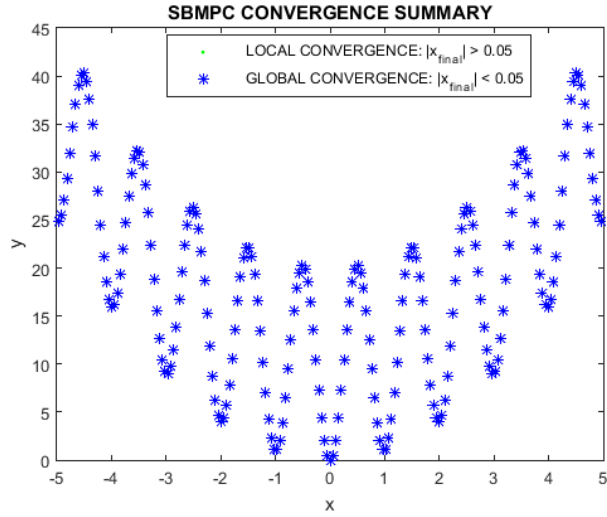


(b)

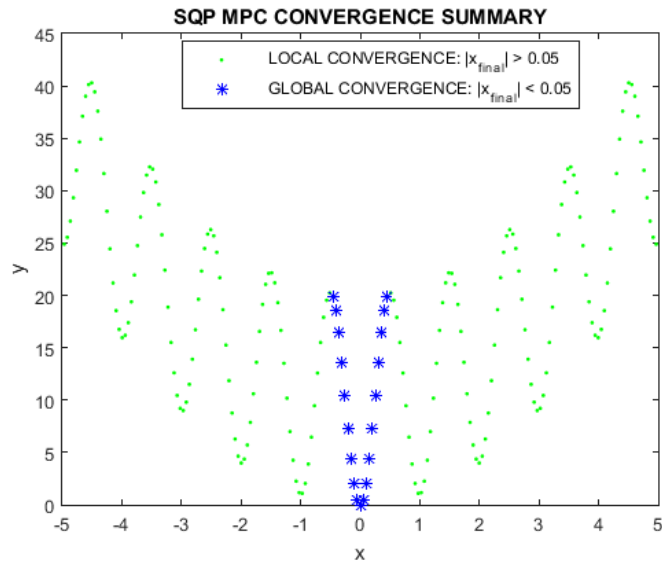
Figure 11. PIV Visualization Uncontrolled and Controlled Cases: angle of attack  $22^\circ$ , velocity 11 m/s. The PIV data in (a) was collected with the control system off, the data in (b) was collected with the control system set to maximize  $Z_{lift}$ , and the tunnel speed corresponds to a Reynolds number of 150,000 based on chord length. The white dashed line indicates zero horizontal velocity  $V_x$ .



*Figure 12. Rastrigin's Function in One Dimension. This objective function with several local minimum points serves as a transparent example for evaluating nonlinear optimization.*



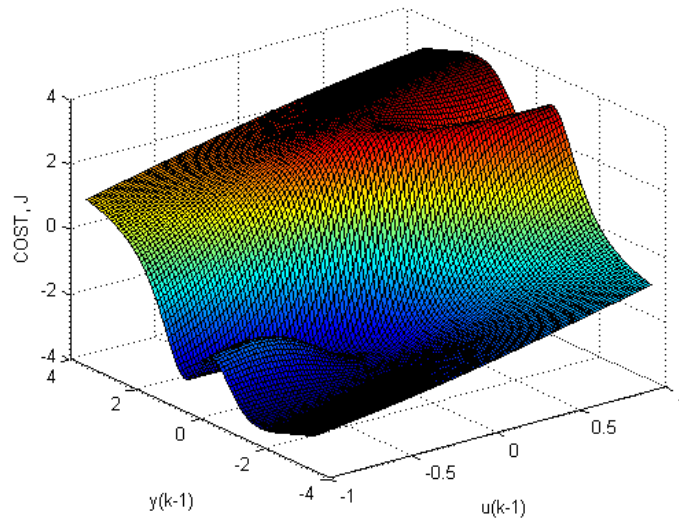
(a)



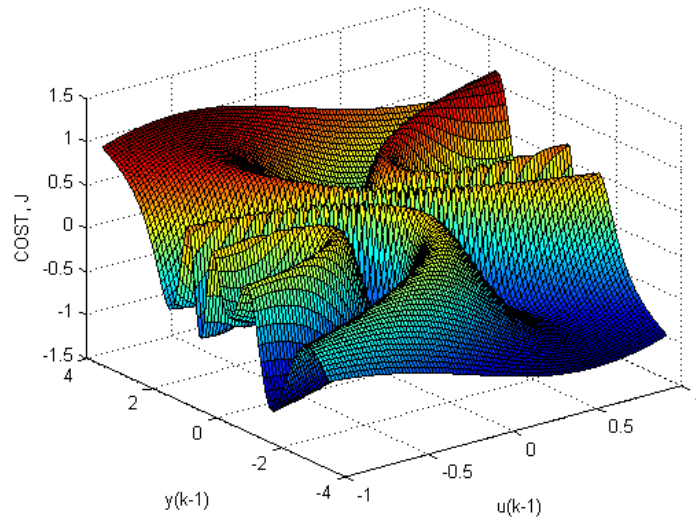
(b)

Figure 13. MPC Convergence Behavior Summary. Each data point represents a unique initial state. Initial configurations for which the simulation converges to within a small region about the global minimum are marked with a blue asterisk, while initial configurations for which the simulation converges to a local minimum are marked with a green dot. With SBMPC, the global minimum is found from every initial state. SQP MPC only finds the global minimum when the initial state is near the global minimum.



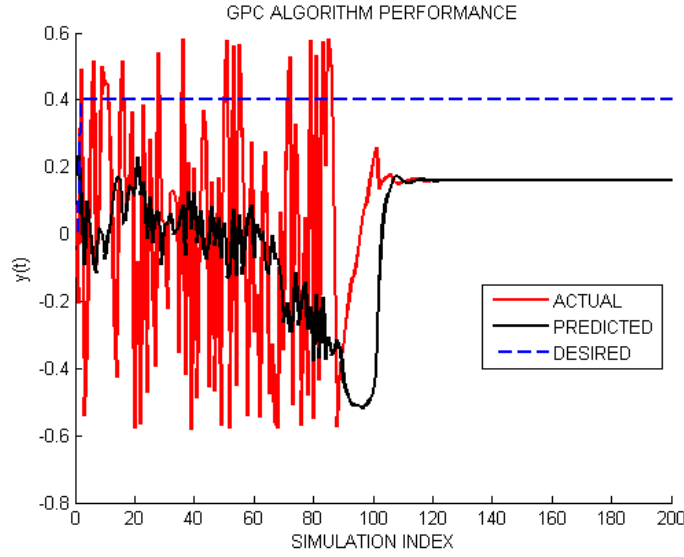


(a)

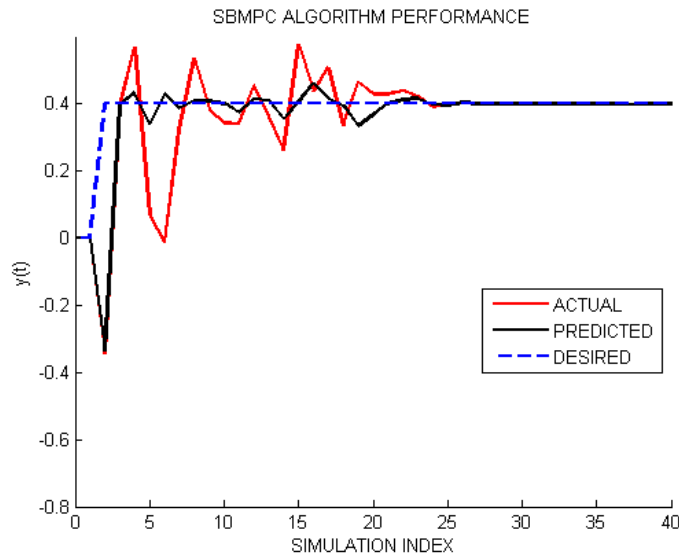


(b)

Figure 14. Benchmark Plant Visualization. Plot (a) is for  $\beta = 1.0$ , and plot (b) for  $\beta = 0.2$ . By modifying  $\beta$ , the number of occurrences of local minima in the state space may be greatly increased. In both plots, the prediction horizon  $N = 1$ .



(a)



(b)

Figure 15. Benchmark Results:  $\beta = 0.2$ , step tracking. After a 90-second training phase, the reference was tracked using GPC (a) and SBMPC (b). Both converge more slowly than in the previous case. However Neural GPC convergence takes 100 simulation steps while the Adaptive SBMPC method converges within 20 steps. The GPC suboptimal convergence state is due to finding a local minimum. The error plot (c) indicates a difference of 2.5 orders of magnitude between globally optimal convergence of SBMPC and the locally optimal convergence of GPC.

Time (s)	Description	Quantitative Changes
0 to 5000	Normal boiler operation	None
500 to 1000	Constricted air flow	$\Phi_{\max}$ is 36% smaller
1000 to 1500	Damp fuel	H <sub>2</sub> O added to comprise 5% of fuel mass
1500 to 2000	Smaller chamber volume	15% reduction in volume

Figure 16. Time Variation of Simulation Plant Dynamics for the Power System Combustion Control Problem. Every 500 sec the plant dynamics were substantially changed.

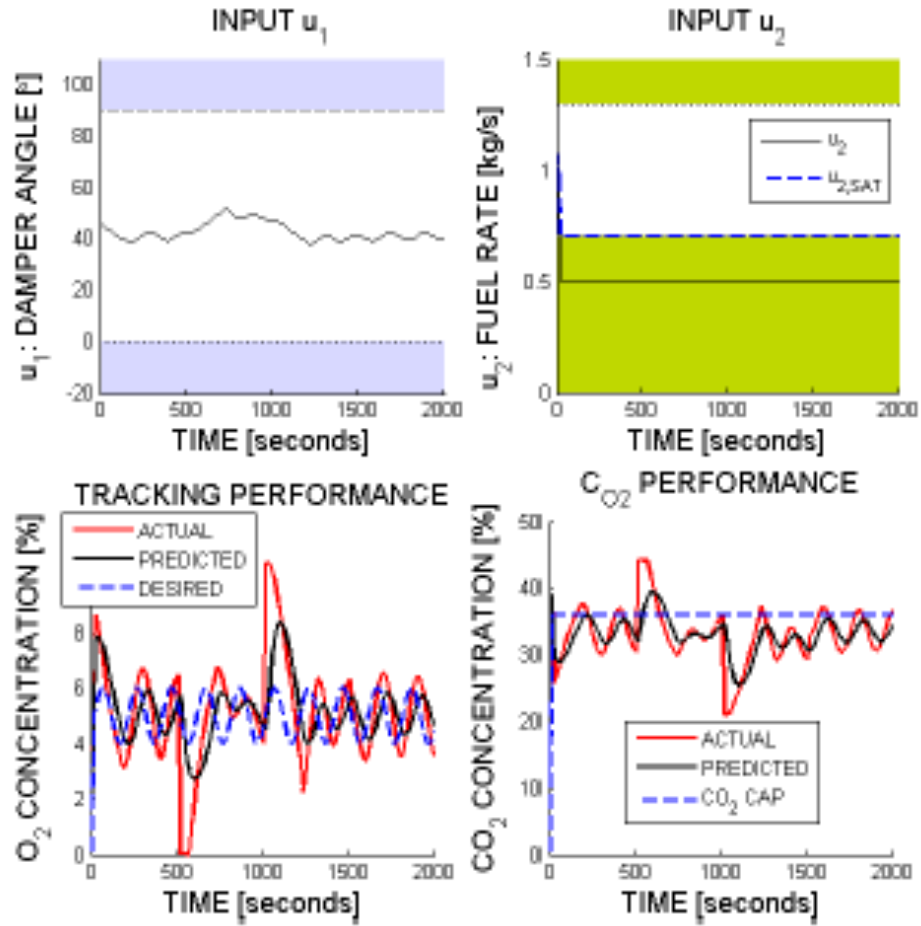


Figure 17. Neural GPC Power Plant Combustion Control Results. With plant changes occurring every 500 seconds, the model adapts and control inputs are updated simultaneously. The shaded upper and lower regions on the input plots are infeasible regions beyond the input constraints. The value  $u_{2,SAT}$  is input to the plant when the fuel rate constraint violation occurs. Because of this saturation of  $u_2$ , tracking is unsuccessful as  $u_1$  alone lacks the control authority to track the reference.

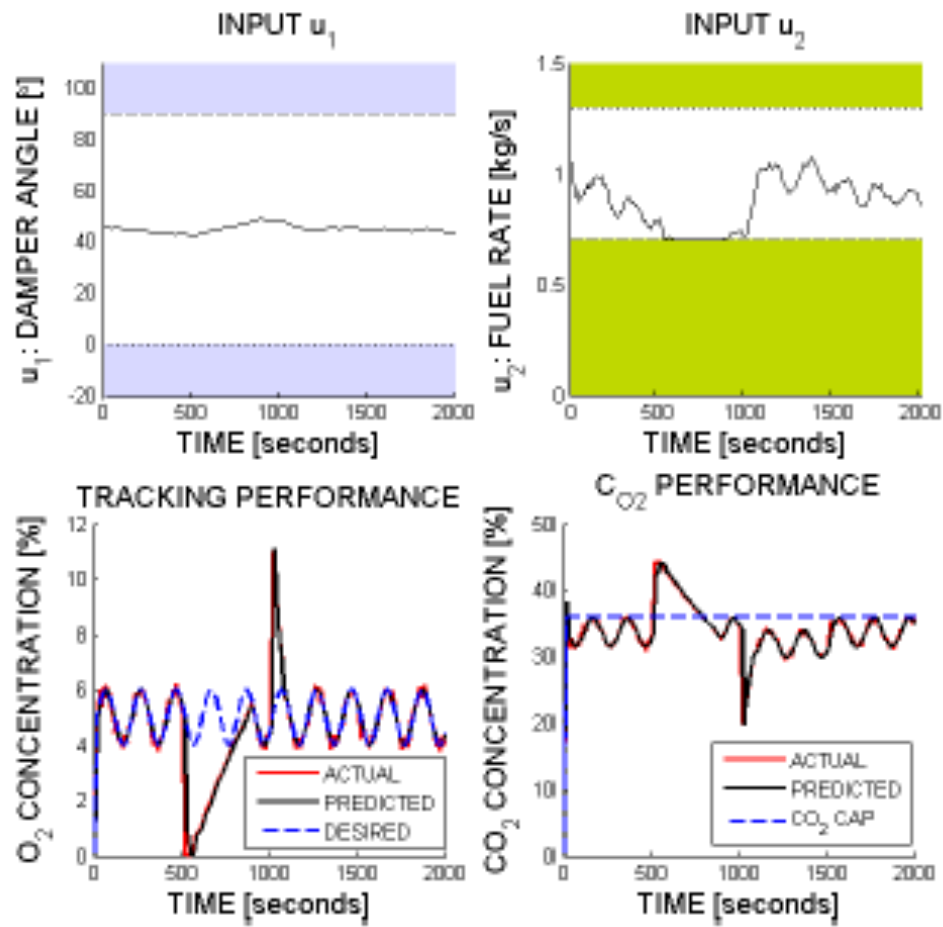


Figure 18. SBMPC Power Plant Combustion Control Results. SBMPC successfully adapts to the plant changes at 500 second intervals, and once converged, low tracking error and output constraint satisfaction is achieved.